الجمهورية الجزائرية الديمقراطية الشعبية

DEMOCRATIC AND POPULAR ALGERIAN REPUBLIC

وزارة التعليم العالي والبحث العلمي

MINISTRY OF HIGHER EDUCATION AND SCIENTIFIC RESEARCH

جامعة الشهيد حمه لخضر الوادي

ECHAHID HAMMA LAKHDAR UNIVERSITY OF EL-OUED

كلية التكنولوجيا

Faculty of Technology

قسم الهندسة الكهربائية

Departement of Electrical Engineering

Master 's Thesis

In order to obtain an Academic Master's diploma in Technology

Specialty: Electrical control

Theme

Comparative PV Model Identification from Experimental Data Using PSO

Presented by:

ABID Mohammed Amine
GUERMIT Nassim

Jury Members:

President:	**Dr. Touil Sliman**	**MCA**	**El-Oued University**
Examiner:	**Dr. Toumi Djaafar**	**MCA**	**El-Oued University**
Supervisor:	**Dr. Bechouat Mohcene**	**MCA**	**El-Oued University**
Co-Supervisor:	**Dr. Kaid Imadeddine**	**MCA**	**El-Oued University**

University year: 2025/2026

الجمهورية الجزائرية الديمقراطية الشعبية

DEMOCRATIC AND POPULAR ALGERIAN REPUBLIC

وزارة التعليم العالي والبحث العلمي

MINISTRY OF HIGHER EDUCATION AND SCIENTIFIC RESEARCH

جامعة الشهيد حمه لخضر الوادي

ECHAHID HAMMA LAKHDAR UNIVERSITY OF EL-OUED

كلية التكنولوجيا

Faculty of Technology

قسم الهندسة الكهربائية

Departement of Electrical Engineering

Master 's Thesis

In order to obtain an Academic Master's diploma in Technology

Specialty: Electrical control

Theme

Comparative PV Model Identification from Experimental Data Using PSO

Presented by:

ABID Mohammed Amine
GUERMIT Nassim

Jury Members:

President:	**Dr. Touil Sliman**	**MCA**	**El-Oued University**
Examiner:	**Dr. Toumi Djaafar**	**MCA**	**El-Oued University**
Supervisor:	**Dr. Bechouat Mohcene**	**MCA**	**El-Oued University**
Co-Supervisor:	**Dr. Kaid Imadeddine**	**MCA**	**El-Oued University**

University year: 2025/2026

بسم الله الرحمن الرحيم

DEDICATION

All praise and gratitude are due to Allah, who granted me the strength, guidance, and perseverance to complete this work. To Him belongs all praise, from beginning to end.

I dedicate this work to my beloved grandmother, in appreciation of her precious place in my life and for her continuous encouragement and support throughout my academic journey.

To my dear parents, with deepest gratitude for their endless sacrifices, unwavering support, and constant encouragement. Their love and dedication have been the foundation of every achievement in my life.

To my brothers and sisters, who are my joy, pride, and happiness, and whose presence has always been a source of strength and inspiration.

To my dear uncle, in recognition of his support and willingness to lend a helping hand whenever it was needed.

I also dedicate this work to everyone who supported, encouraged, and contributed to its completion through a kind word, valuable advice, or sincere assistance, including my friends, colleagues, and teachers.

May this effort be a source of beneficial knowledge and a positive legacy that endures beyond its author.

MOHAMMED AMINE

DEDICATION

All praise and gratitude are due to Almighty God, whose blessings, guidance, and mercy enabled me to complete this work and pursue the path of knowledge and learning.

I dedicate this work to:

My beloved mother, whose endless prayers, sacrifices, and unwavering support have been a constant source of strength throughout my journey.

My dear father, whose guidance, encouragement, and steadfast presence have always inspired me, especially during moments of difficulty.

My brothers and sisters, my source of support, pride, and companionship in life.

My teachers, friends, and everyone who stood by my side.

To those who never hesitated to offer a word of encouragement, a gesture of support, or sincere advice; and to all who left a positive mark on my journey and motivated me to move forward, even by a single step.

This work is dedicated to you all, with deep gratitude and appreciation for your sincere support and kindness.

NASSIM

ACKNOWLEDGMENTS

In the name of Allah, the Most Gracious, the Most Merciful.

We extend our deepest gratitude and praise to Allah Almighty, who granted us the strength, perseverance, and determination to complete this work. To Him belongs all praise and thanks, from beginning to end.

We would also like to express our sincere appreciation to our supervisor Dr. BECHOUAT mohcene, for his valuable guidance, insightful advice, and continuous support throughout this research. His dedication, time, and efforts greatly contributed to the successful completion of this work.

We would also like to extend our heartfelt thanks to everyone who contributed, directly or indirectly, to the realization of this study, and to all those who provided assistance, encouragement, or valuable advice during our academic journey.

Our sincere gratitude also goes to all our teachers and professors who contributed to our academic and personal development, and to everyone who supported and assisted us throughout the different stages of this work.

Finally, we pray that this effort will be accepted by Allah and that it may serve as beneficial knowledge for all who make use of it.

ABSTRACT

This thesis presents a comparative study of photovoltaic (PV) model identification using experimental current-voltage (I-V) data and Particle Swarm Optimization (PSO). The primary objective is to accurately extract the unknown parameters of different PV equivalent circuit models-namely the ideal model (IM) and single-diode model (SDM) and double-diode model (DDM)-based on real experimental measurements. The experimental data were collected from a PV panel installed at the Research Unit in Renewable Energies (URAER) in Ghardaia, Algeria, under natural operating conditions. The PSO algorithm is employed as a global optimization tool to minimize the mean square error (MSE) between the measured and simulated current values for each model. A comparative analysis is conducted to evaluate the accuracy, convergence behavior, and computational efficiency of IM ,SDM and DDM when identified using the same experimental dataset and the same PSO configuration. Simulation results, carried out in the MATLAB environment, show that while both models achieve good agreement with experimental data, the double-diode model provides slightly higher accuracy, particularly at low irradiance levels, at the cost of increased computational complexity. The findings of this study offer practical guidance for selecting the most appropriate PV model and PSO-based identification strategy depending on the required trade-off between precision and computational effort.

Keywords: Photovoltaic cell model, Particle Swarm Optimization (PSO), parameter extraction, current-voltage (I-V) curve, equivalent circuit models (single/double-diode).

الملخص

تُقدم هذه الأطروحة دراسة مقارنة لتعرّف نموذج الخلية الكهروضوئية (PV) باستخدام بيانات التيار-الجهد (I-V) التجريبية وخوارزمية تحسين سرب الجسيمات (PSO) الهدف الأساسي هو استخراج المعاملات غير المعروفة بدقة لنماذج دوائر كهروضوئية مكافئة مختلفة-وهي النموذج المثالي (IM) و نموذج الديود المفرد (SDM) ونموذج الديود المزدوج (DDM) بناءً على قياسات تجريبية حقيقية. تم جمع البيانات التجريبية من لوح كهروضوئي مثبت في وحدة الأبحاث في الطاقات المتجددة (URAER) بغرداية، الجزائر، تحت ظروف تشغيل طبيعية. تم استخدام خوارزمية PSO كأداة تحسين شاملة لتقليل متوسط مربع الخطأ (MSE) بين قيم التيار المقاسة والمحاكاة لكل نموذج. تم إجراء تحليل مقارن لتقييم الدقة وسلوك التقارب والكفاءة الحسابية لنماذج IM, SDM و DDM عند تعرّفهما باستخدام نفس مجموعة البيانات التجريبية ونفس إعدادات .PSO أظهرت نتائج المحاكاة، التي نُفذت في بيئة MATLAB، أنه على الرغم من تحقيق النماذج لتوافق جيد مع البيانات التجريبية، فإن نموذج الديود المزدوج يقدم دقة أعلى قليلاً، خاصةً عند مستويات الإشعاع المنخفض، وذلك على حساب زيادة التعقيد الحسابي. تقدم نتائج هذه الدراسة توجيهاً عملياً لاختيار النموذج الكهروضوئي الأنسب واستراتيجية التعرّف القائمة على PSO وفقاً للمفاضلة المطلوبة بين الدقة والجهد الحسابي.

الكلمات المفتاحية: نموذج الخلية الكهروضوئية، خوارزمية تحسين سرب الجسيمات(PSO) ، استخراج المعاملات، منحنى التيار-الجهد(I-V) ، النماذج المكافئة (أحادي/ثنائي الديود).

List of figures

List of tables

List of contents

CHAPTER II

Photovoltaic System Identification

CHAPTER III

Experimental results and simulation

General Introduction

General Introduction

Renewable energies, particularly photovoltaic (PV) solar energy, have become a central pillar in the global transition toward sustainable and environmentally friendly power generation. Algeria, with its exceptional solar potential—especially in the Saharan regions-offers a unique and promising environment for the development and optimization of PV systems. However, the performance of a photovoltaic system is inherently linked to the accuracy of the mathematical models used to represent its electrical behavior under real operating conditions. These models, such as the ideal model (IM) and the single-diode model (SDM) and double-diode model (DDM), contain nonlinear parameters that must be precisely identified to ensure reliable simulation, fault diagnosis, and maximum power point tracking.

This thesis focuses on the comparative identification of PV model parameters using experimental current-voltage (I-V) data collected from an LX-100M photovoltaic panel installed at the Research Unit in Renewable Energies (URAER) in Ghardaïa, Algeria. To overcome the limitations of traditional numerical methods—such as sensitivity to initial guesses and complex gradient calculations—we employ the Particle Swarm Optimization (PSO) algorithm, a robust metaheuristic technique inspired by swarm intelligence.

The primary objective is to evaluate and compare the accuracy, convergence behavior, and computational cost of the IM and SDM and DDM when identified under identical experimental conditions (same dataset and same PSO configuration). A comparative analysis is conducted based on the mean square error (MSE) between measured and simulated current values for each model. This work aims to provide practical guidance for selecting the most appropriate PV model and parameter extraction strategy based on the desired trade-off between precision and computational effort. Simulation results, carried out in the MATLAB environment, are presented and discussed to support these findings.

CHAPTER I

Modeling of Photovoltaic Systems

I.1 Introduction

In this chapter, we will discuss renewable energies in general and photovoltaic solar energy in particular. We will learn about the working principle of a photovoltaic cell, its description, types, performance, and characteristics, along with a model of it.

Photovoltaic solar energy is one of the most sustainable and widely used forms of energy. The sun is a natural source of energy that produces virtually limitless power. This energy relies on photovoltaic cells, which convert photons of light from the sun, as they collide with electrons in the solar panel, into direct current. This current is then converted into electricity, which we utilize in numerous applications **[1]**.

I.2 Renewable energies

Renewable energy sources are natural, sustainable, and environmentally friendly. Examples include:

- **Solar energy:** utilizing heat and light.
- **Wind energy:** using wind turbines.
- **Hydropower:** utilizing the movement and flow of water.
- **Geothermal energy:** utilizing the Earth's heat.
- **Bioenergy:** using organic materials and plants.

I.3 Origin of solar energy

Solar energy is produced by the fusion that occurs in the sun's core, which is composed of approximately 74% hydrogen, 24% helium, and 2% oxygen, carbon, iron, and neon **[1]**. Hydrogen atoms are converted into helium through nuclear fusion, a process described by Albert Einstein's equation $E=mc^2$, where mass is converted into energy. This reaction takes place at temperatures exceeding 15 million Kelvin. The solar energy produced by this reaction is then converted into light radiation that spreads in all directions. This radiation reaches the Earth's surface with a density constant of approximately 1367 W/m^2 after traveling a vast distance of 150 million kilometres in about 8 minutes **[2]**.

I.4 The solar panel

A solar panel is a flat device made of a semiconductor material called silicon and contains many solar cells connected together. It works by receiving photons of light from the sun and converting them into electrons, then into direct current, which we use for various purposes. The dimensions of a solar panel vary depending on the type and application.

I.5 Solar radiation

The sun produces radiation that we classify as follows **[3]** :

Total radiation: This is the sum of all radiation reaching the Earth's surface and is divided into direct radiation, diffuse radiation, and reflected radiation.

Direct radiation: This is radiation that reaches the Earth's surface directly from the sun without being affected by any other medium.

Diffuse radiation: This is radiation that reaches the Earth after interacting with clouds and the atmosphere as a whole.

Reflected radiation: This is radiation that is reflected from the Earth's surface or objects on the Earth's surface.

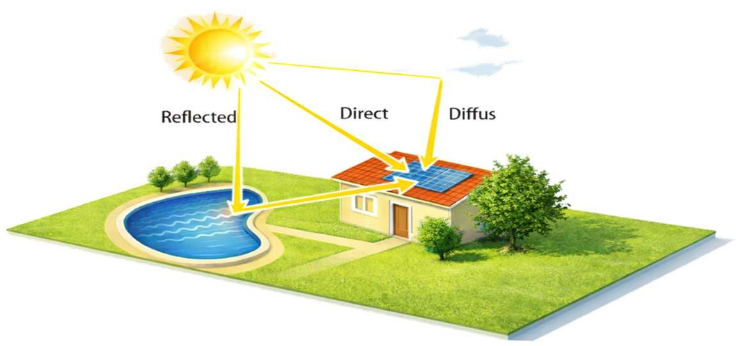

Figure I.1: Types of solar radiation

I.6 Photovoltaic cell

The photovoltaic cell is the smallest unit in a solar panel's structure and is made of a semiconductor material, silicon. A photovoltaic cell consists of two layers of chemically treated silicon **[4]**. The top layer (N-type) is made of silicon with added phosphorus, which has more electrons than silicon, resulting in an excess of free electrons and making the layer negatively charged. The bottom layer (P-type) is also made of silicon with added boron, which has fewer electrons than silicon, creating holes that need electrons to make the layer positively charged.

I.6.1 Photovoltaic cell manufacturing technologies

Cells vary depending on the material they are made from. Silicon, in both its crystalline and amorphous forms, is the most widely used material worldwide. It is a tetravalent semiconductor. Other semiconductors include gallium arsenide (GaAs), cadmium telluride (CdTe), and indium phosphide (InP), among others.

I.6.2 Principle of operation of a photovoltaic cell

The process is called the photoelectric effect, where photovoltaic cells absorb sunlight (photons). When a photon strikes a molecule, it releases electrons from its atoms, producing negative charges (electrons) and positive charges (holes). This creates an electric field (P-N junction) between the two layers. This field separates and distinguishes the charges, pushing electrons towards the negative (N-type) layer and holes towards the positive (P-type) layer. As a result of this separation, these free electrons seek an outlet. They escape through fine metal lines that collect the electrons and transport them out through the connecting wires. In short, the process begins with the absorption of sunlight, which releases electrons, producing positive charges (holes) on one side and negative charges (electrons) on the other. This separation creates a vacuum or electric field. This field acts as a barrier, preventing incoming electrons from combining with the holes and hindering the random scattering of electrons **[5]**.

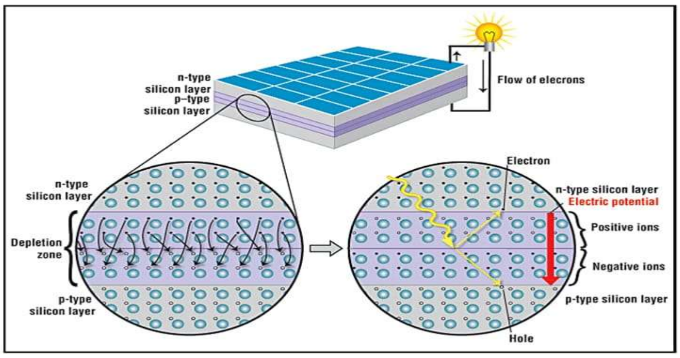

Figure I.2: Principle of operation of a photovoltaic cell

I.6.3 Types of photovoltaic cells

There are several types of photovoltaic cells, differing in cost, efficiency, and features. However, their efficiency remains very low, ranging between 8% and 23%. Currently, there are three main types of these cells **[6]**.

Monocrystalline cells: [1]

- Its color is dark black.
- Very pure crystals are required.
- High efficiency solar panels (16-24%).
- It performs better in high temperatures and low light conditions.
- It is considered best for limited spaces such as homes.
- It is the most expensive and longest-lasting option.
- It produces more waste.

Figure I.3: Monocrystalline photovoltaic cell**.**

Polycrystalline cells:

- It is blue in color and consists of several crystals**.**
- It is less expensive and slightly less efficient (15-18%) **[7]** .
- It has a long lifespan, is slightly affected by high temperatures, and requires a larger area.
- It is used in homes, projects, and stations.

Figure I.4: Polycrystalline photovoltaic cell**.**

Amorphous cells (Thin film):

- Its production rate is low (8-13%) **[8]**.
- its cost is very low, and it works even in low light.
- The layer is very thin and flexible.
- It has the shortest lifespan among other types and is used in small devices such as calculators and remote controls.

Figure I.5: Amorphous photovoltaic cell**.**

I.7 Photovoltaic field

A photovoltaic field consists of a large number of solar panels. These fields require a vast, consistently sunny area to feed into an electrical grid. This is what is called a power generation station.

Figure I.6: Photovoltaic field

I.8 Photovoltaic systems

The installation and operation of solar panels vary depending on the application, and there are three types of photovoltaic systems **[9]**.

Grid-connected systems: These systems are connected to the public grid and are considered a renewable form of energy. They do not require batteries and cease operation when the electricity supply is interrupted.

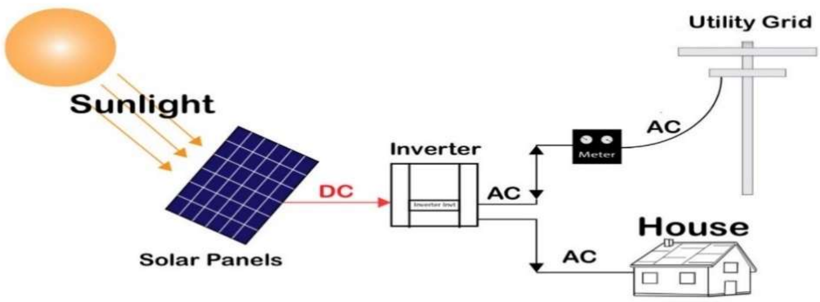

Figure I.7: Example of Grid-connected systems.

Off-grid systems: These systems are found in remote and isolated areas not connected to the public grid. They rely on batteries for energy storage.

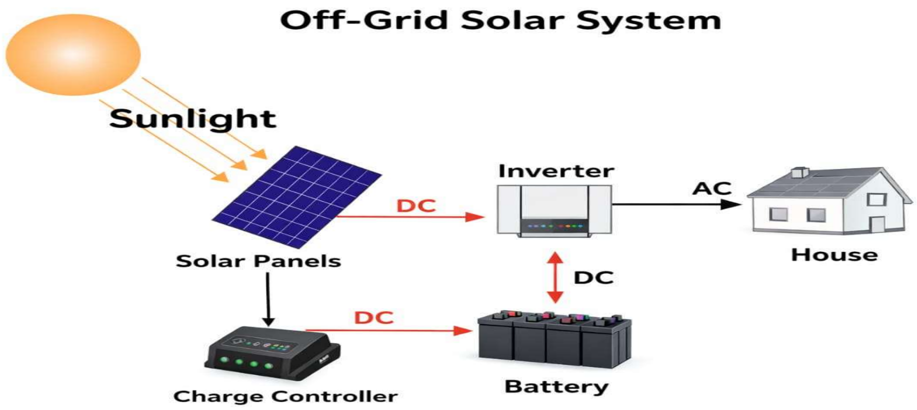

Figure I.8: Example of Off-grid systems.

Hybrid system: It may combine several systems such as connected and independent, and even other forms of energy such as wind and water... This system is considered the most expensive, the most demanding, and the most efficient.

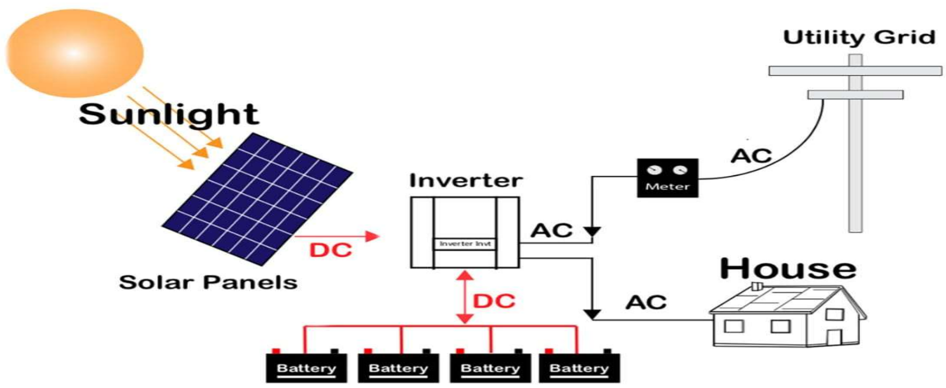

Figure I.9: Example of Hybrid systems.

I.9 Connecting of photovoltaic cells:

Regrouping in series:

In a series group, the cells are crossed by the same current and the resultant characteristic of the series group (index S) is obtained by the addition of the voltages at the given current .the figure shows the resulting characteristic (Vs,I_{cc}) obtained by associating in series Ns identical cells .

$$V_s = N_s . V_{CO} \quad \textbf{(I.1)}$$

To for general expression :

$$I_{cc} = I_c \qquad \textbf{(I.2)}$$

With V_C : voltage supplied by a cell. For this grouping, the current is common to all the cells.

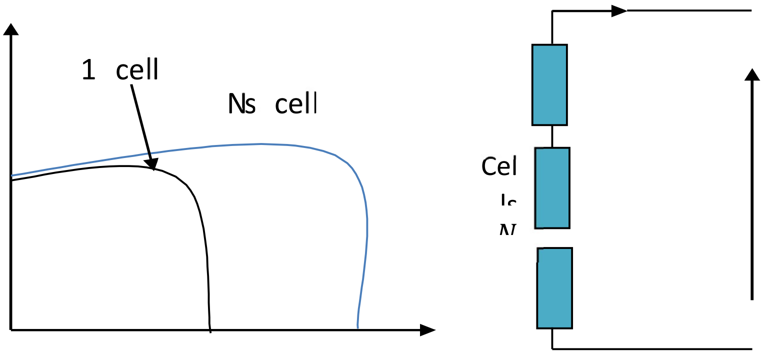

Figure I.10 : Current voltage characteristic of (N_s) cells in series **[8]**.

Regrouping in parallel:

Paralleling allows the output current to be increased. For a group of cells connected in parallel, the output current has the general expression:

$$I_s = N_p \, . \, I_{cc} \qquad \textbf{(I.3)}$$

With I_{cc} : current supplied by a cell.

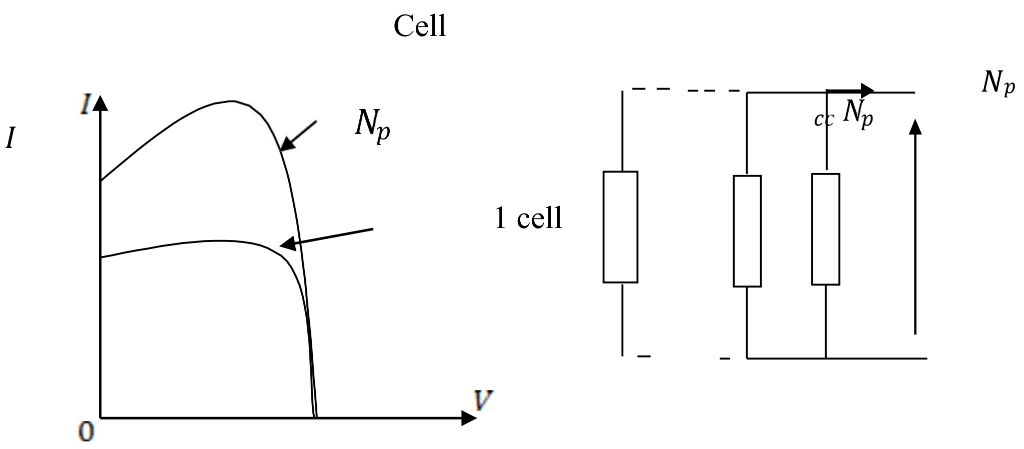

Figure I.11: Current voltage characteristic of (Np) cell in Parallel **[8]**.

I.10 Equivalent diagram of a photovoltaic cell

I.10.1 Simple diode :

A.1 Ideal photovoltaic cell (Real model)

The solar cell is a semiconductor component which delivers a current by exciting it with photons, so as a first approximation we have a current source short-circuited by a diode (because the solar cell is a PN junction) **[11]**.

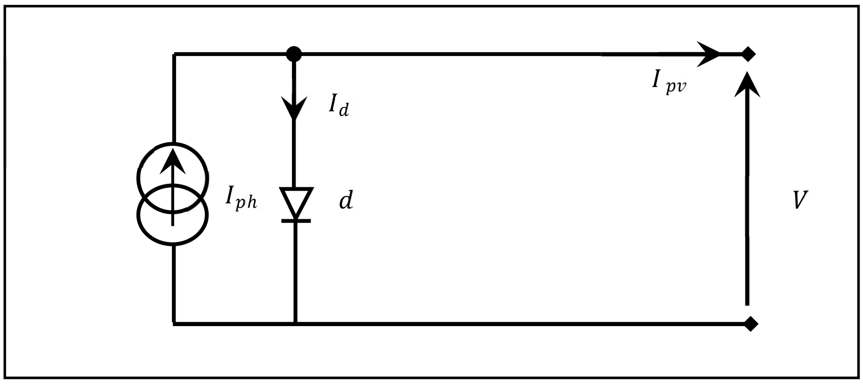

Figure I.12: Model of an ideal photovoltaic cell **[12]**.

The current delivered by the photovoltaic cell according to the law of knots:

$$I_{pv} = I_{ph} - I_d \quad \textbf{(I.4)}$$

- $\boldsymbol{I_{pv}}$: Current supplied by the cell.
- $\boldsymbol{I_{ph}}$: The photon current which is estimated by $\boldsymbol{I_{cc}}$.(generated photo-current).
- $\boldsymbol{I_d}$: The parallel current through the diode (Current through the diode).

For an ideal $\boldsymbol{P_v}$ generator, the voltage across the load resistor is equal to the voltage across the diode:

$$\boldsymbol{V = V_d} \quad \textbf{(I.5)}$$

$$I_d = I_s(exp\,\frac{V_d}{V_t}) - 1 \quad \textbf{(I.6)}$$

$\boldsymbol{I_s}$: The reverse saturation current of the diode [A]

$\boldsymbol{V_d}$: The voltage across diode D

$\boldsymbol{V_t}$: Thermal potential. According to the replacement of $\boldsymbol{I_{pv}}$

$$I_{pv} = I_{ph} - I_s(exp\,\frac{V_d}{V_t}) - 1 \qquad \textbf{(I.7)}$$

A.2 Solar cell with series resistance:

This model is called (1M4P)

Add the series resistance $\boldsymbol{R_s}$ as 4th parameter

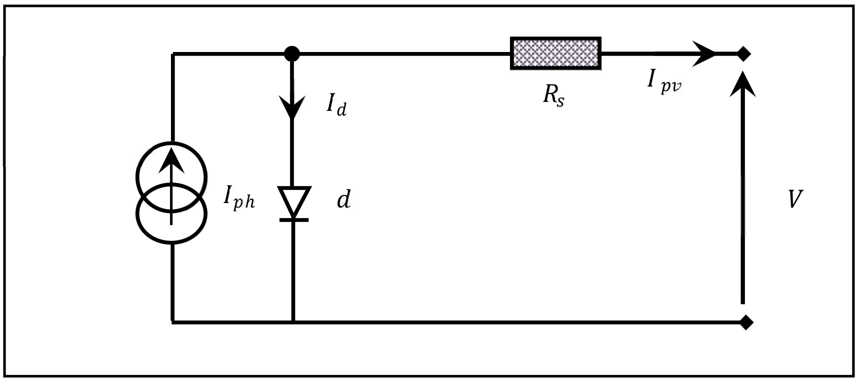

Figure I.13: Model (1M4P) **[12]**.

$\boldsymbol{R_s}$**:** represents the resistance of the connections and $\boldsymbol{V_d}$ will be:

$$V_D = V + R_S.I_{RS} \qquad \textbf{(I.8)}$$

$$I_D = I_S(e^{\frac{V_{pv}+R_S I_{pv}}{nkt}} - 1) \qquad \textbf{(I.9)}$$

Under normal irradiance conditions **(1000 W/m²)** and temperature **(25 c)**

$$\frac{KT}{q} = 26mv \qquad \textbf{(I.10)}$$

$$K = 1.38 * 10^{-23} j.k^{-1} \qquad \textbf{(I.11)}$$

$$T = 25 + 273 = 298k \qquad \textbf{(I.12)}$$

$$e = 1.16*10^{-19}c \qquad \textbf{(I.13)}$$

So, the relationship becomes:

$$I_{pv} = I_{ph} - I_{sat}(eq\frac{v + I_{rs}}{nK_T} - 1) \quad \textbf{(I.14)}$$

I.10.2 Photovoltaic cell Modeling (Single diode)

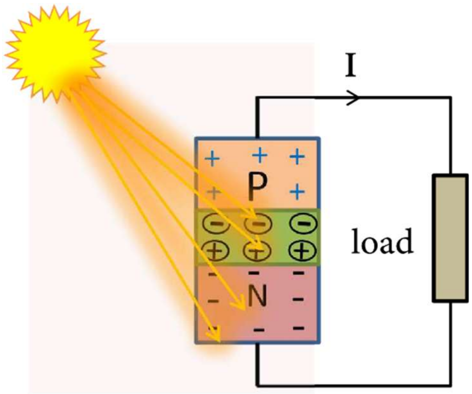

Figure I.14: Principle of operation of a photovoltaic cell (PN junction) under solar illumination **[6].**

$$I = I_{PH} - I_D - I_{sh} \quad \textbf{(I.15)}$$

$$I_d = I_s(e^{nVT} - 1) \quad \textbf{(I.16)}$$

$$I = I_{ph} - I_s\left(e^{\frac{I_{Rs}}{nV_T}} - 1\right)\mathrm{V} + \frac{I_{RS}}{R_{sh}} \quad \textbf{(I.17)}$$

Five parameter model: **I_{PH}, I_S, n, R_S, R_{SH}**

$V_T = \frac{KT}{q}$ is the thermal

voltage (=25mV at 25 °C) where k is the Boltzmann constant, T is the absolute temperature of the pn junction, and q is the electron ch

$\boldsymbol{I_{ph}}$ = light proportional generated current.

$\boldsymbol{I_s}$ = diode reverse saturation current .

$\boldsymbol{n}$ = ideality (quality) factor.

$\boldsymbol{R_s}$ = equivalent series resistance.

$\boldsymbol{R_{sh}}$ = equivalent shunt (parallel) resistance arge.

I.10.3 Photovoltaic cell Modeling (Double diode)

$$I = I_{Ph} - I_{d1} - I_{d2} - I_{sh} \quad \textbf{(I.18)}$$

$$I_d = I_s(e\frac{v_d}{nV_T} - 1) \quad \textbf{(I.19)}$$

$$I \quad = I_{ph} - I_{s1}(e\frac{V + IR_S}{n_1 V_T} - 1) - I_{s2}(e\frac{V + IR_S}{n_2 V_T} - 1) \quad \textbf{(I.20)}$$

Seven parameter model: I_{PH}, I_{S1}, I_{S2}, n_1, n_2, R_s, R_{sh}.

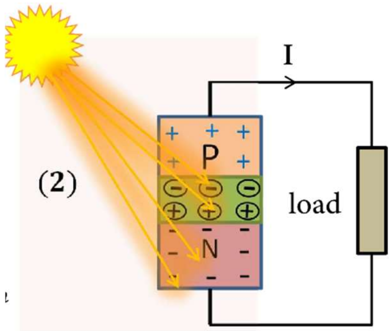

Figure I.15: Physical principle of a solar cell and current generation in the PN junction.

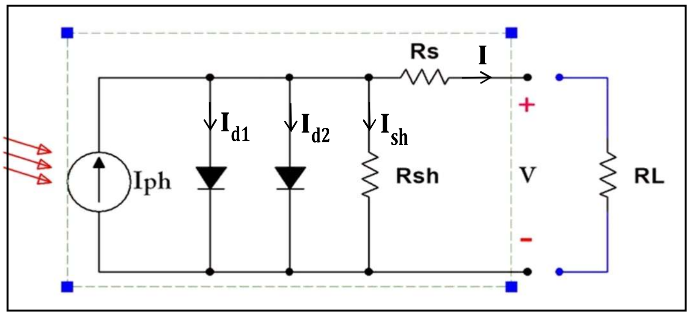

Figure I.16: Equivalent circuit diagram of a photovoltaic cell (Double Diode Model)

Characteristics of the single diode model

$$I = I_{PH} - I_D - I_{SH} \quad \textbf{(I.21)}$$

$$I = I_{PH} - I_S(e^{I_{RS}nV_T - 1}) - v + I_{RS}R_{sh} \quad \textbf{(I.22)}$$

If we let R_s= 0 and R_{sh} = infty then

$$I = I_{ph} \; - \; I_s(e^{VnV_T} \; - \; 1) \quad \textbf{(I.23)}$$

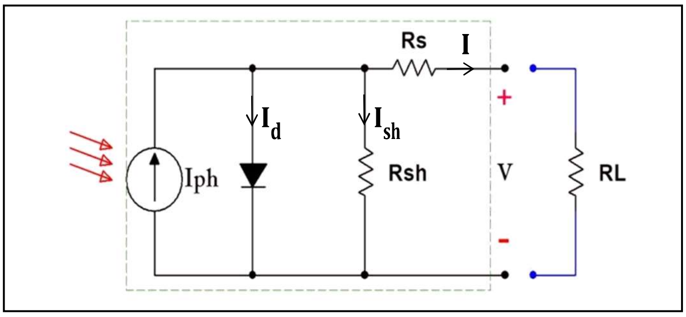

Figure I.17: Equivalent circuit diagram of a photovoltaic cell (Two-Diode Model) showing internal resistances and load.

$$V = nVT\ ln(I_{ph} - \frac{I}{I_s} + 1) \quad \textbf{(I.24)}$$

PV cell can also be characterized by its short circuit current $\boldsymbol{Isc}$ and open circuit voltage $\boldsymbol{Voc}$. $\boldsymbol{Isc}$ can be approximated from eq (3) by setting V = 0 .

$$\boldsymbol{I_{SC} = I_{ph} - I_{s1} - 1 = I_{ph}} \quad \textbf{(I.25)}$$

$\boldsymbol{Voc}$ can be approximated from eq (4) by setting $\boldsymbol{I} = 0$

$$V_{oc} = \frac{nKT}{q}\ ln(\frac{I_{ph}}{I_S}) \quad \textbf{(I.26)}$$

$$P_m(max\ power) = V_m I_m \quad \textbf{(I.27)}$$

$$\eta(\text{efficiency}) = \frac{max\ \ power}{light\ \ power} = \frac{P_m}{P_{in}} \quad \textbf{(I.28)}$$

$$\alpha(fill\ factor) = \frac{P_m}{V_{oc} I_{sc}} \quad \textbf{(I.29)}$$

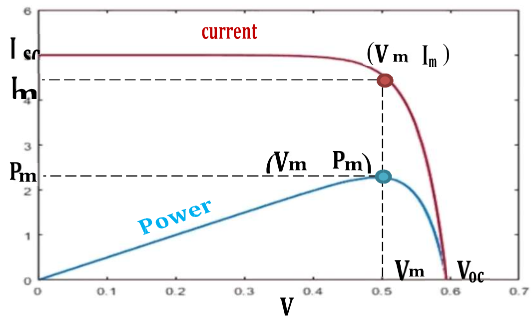

Figure I.18: Characteristic curves of a solar cell (I-V and P-V) and Maximum Power Point (MPP) identification.

Conclusion

In this chapter, we covered the main fundamentals of photovoltaic energy, from the working principle and different types of solar cells (monocrystalline, polycrystalline, thin-film), to their connection methods, and finally to mathematical modeling using single-diode and double-diode models. We also examined their key electrical characteristics such as short-circuit current, open-circuit voltage, and fill factor, providing a solid theoretical foundation for understanding solar panel behavior under various conditions.

Building upon these theoretical foundations, the next section will focus on the identification of photovoltaic parameters. We will explore various extraction methods, specifically the Newton-Raphson method as a numerical iterative technique, and the Particle Swarm Optimization (**PSO**) algorithm as a metaheuristic approach. This transition aims to accurately determine cell parameters and develop a robust model that effectively simulates real-world behavior.

CHAPTER II

Photovoltaic System Identification

II.1. Introduction

Electricity creation with the help of the photovoltaic (PV) result has many advantages. One of these advantages is associated to the decrease of the greenhouse effect, and this unusual benefit makes this electricity generation technology measured one of the environmentally friendly technologies. The temperature of the earth is the effect of the stability between the energy released from the earth to space and the received radiation by the sun. The return radiation from the Earth to the atmosphere has been deeply influenced by the existence and arrangement of the Earth's atmosphere. The sunlight that reaches the earth warms the atmosphere and the surface of the earth.

Consequently, the Earth's atmosphere radiates its heat in the form of infrared radiation. These reflections are reabsorbed by many gases, including carbon dioxide, methane, and various types of chlorofluorocarbons (CFCs), and heat the atmosphere6. This trapping of heat is similar to the greenhouse effect, which is why this process is called the greenhouse effect. Available evidence offers that levels of CO_2 will be doubled by 2030, making global warming between 1 and 4 °C.

This leads to changes in wind and rainfall patterns, which in turn might make the Earth's oceans rise and the continents dry out. About 85% of the total greenhouse warming on the earth's surface is due to water vapor in the atmosphere and 12% to greenhouse gases. It is clear that the concern is not about the increase of water vapor, but the main concern is about the emission of greenhouse gases, especially carbon dioxide, which is the result of human activities. Activities of humans have extended to a scale that affects the environment of the planet and its appeal to humans. These side effects can be overwhelming, and it is likely technologies that have low ecological influence and without the emission of "greenhouse gases" will become more important in the coming decades. Since the energy sector is the major producer of "greenhouse gases" through the combustion of fossil fuels, technologies such as photovoltaics, which can replace fossil fuels, should be used.

II.2 Identification Methodology

In this section, the principle of system identification is described. Dynamic models depend heavily on the amount of a priori knowledge about the dynamic process that is to be incorporated. Generally, modeling any dynamical system can be categorized into two approaches: first-principal modeling and data-driven modeling **[13]**.

First-principal modeling uses an understanding of the system's physics to derive a mathematical representation, whereas data-driven modeling involves using empirical data to construct a model for the system. The two approaches classify the modeling process in terms of known parameters and structure into black box, grey box, and white box modeling as suggested by Figure II.1.

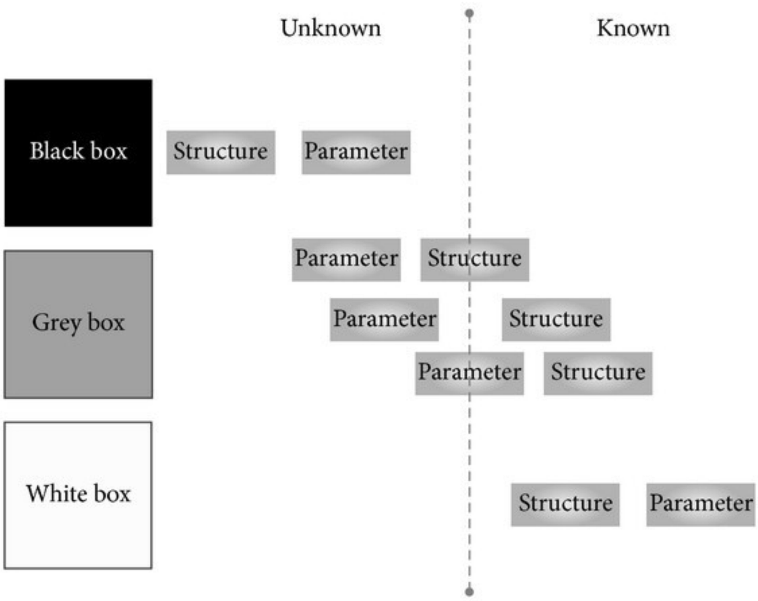

Figure II.1: Classification of dynamical systems by model structure and parameter.

According to white box modeling is when a model is perfectly known; it is possible to construct the model entirely from prior knowledge and physical insight. Grey box modeling is when some physical insight is available, but several parameters remain to be determined from observed data. In black box modeling, no physical insight is available or used, but the chosen model structure belongs to candidate models that are known to have good flexibility and have been successful in the past. **[14]**.

The black box modeling is used for this work. It is usually a trial-and-error process where one estimates the parameters of various structures and compares the results. The PV system constructed and implemented in Figure II.1 is used for data collection purposes. The measured input-output data will then be utilized to select model structure and identify the system.

II.2.1 Newton-Raphson Method

II.2.1.1 Definition

The Newton-Raphson method (often simply called Newton's method), credited to Isaac Newton and Joseph Raphson, serves as a mathematical approach for calculating iterative approximations. It is considered more advantageous than traditional sampling or zero-finding techniques for real-valued functions.

$$x : f(x) = 0 \tag{II.1}$$

This algorithm seeks the minimum or maximum of a given function by identifying the roots (zeros) of its first derivative. This can be accomplished employing various zero-finding techniques (such as the bisection method, false position method, or Newton-Raphson itself), functioning as an optimization algorithm **[23]**.

II.2.1.2 Explanation

The Newton-Raphson approach is an iterative procedure relying on initial estimations and following a structured logical progression to reach a target solution.

The objective is approximated using a tangent line, derived via calculus principles. By calculating where this line intersects the x-axis utilizing basic algebra, a more accurate estimation of the function's root is secured.

This sequence can be executed repeatedly. The quasi-Newton method serves as an advancement of this fundamental process, employing collinear scaling and local quadratic approximations to circumvent the necessity of calculating a complete Hessian matrix. Within this context, novel collinear scaling variables that might seem singular are investigated, introducing an upgraded collinear scaling algorithm that utilizes local quadratic approximation to bolster stability.

Furthermore, the global convergence of this algorithm is mathematically proven. Numerical evaluations involving neural network training with this refined algorithm highlight its enhanced efficiency when juxtaposed with standard algorithms **[14]**.

II.2.1.3 Derivation

In the realm of numerical analysis, Newton's method (or the Newton-Raphson method), named after its creators, is a procedure aimed at discovering increasingly precise approximations for the roots of real-valued functions, as shown in Equation (II.1).

The application of the Newton-Raphson method for a single variable proceeds as follows:

Given a real-valued function f and its corresponding derivative f', determine an initial guess $x0$ for the function's root. Assuming the function meets required mathematical conditions and based on the formula's derivation, $x1$ represents a superior approximation:

$$x_1 = x_0 - \frac{f(x_0)}{f(x_1)} \quad \textbf{(II.2)}$$

From a geometric perspective, the point $(x1, 0)$ marks the x-axis intersection of the tangent line drawn to the function's curve at the coordinate $\boldsymbol{(x0, f(x0))}$.

This iterative cycle continues as: **[15]**.

$$x_{n+1} = x_n - \frac{f(x_n)}{f(x_n)} \quad \textbf{(II.3)}$$

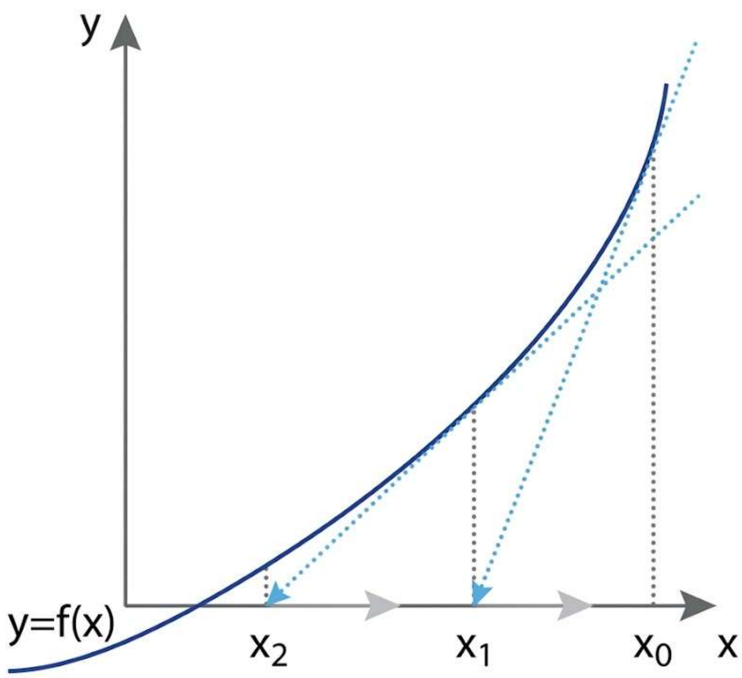

Figure II.2: Illustration of the Newton Raphson Method.

This loop is maintained until a predetermined level of accuracy is achieved.

II.2.1.4. Examples

Calculating a square root **[16]**:

Examine the challenge of determining a number's square root. Newton's method provides one of several approaches to compute this.

For instance, calculating the square root of 612 is mathematically equivalent to resolving:

$$x^2 = 612 \qquad \textbf{(II.4)}$$

Consequently, the function applied in Newton's method becomes:

$$f(x) = x^2 - 612 \qquad \textbf{(II.5)}$$

Its derivative is:

$$f'(x) = 2x \qquad \textbf{(II.6)}$$

Starting with an initial estimate of 10, the progression generated by the method is:

$$x_1 = x_0 - \frac{f(x_0)}{f'(x_0)} = 10 - \frac{10^2 - 612}{2 \times 10} = 35.6 \quad \textbf{(II.7)}$$

$$x_2 = x_1 - \frac{f(x_1)}{f'(x_1)} = 35.6 - \frac{35.6^2 - 612}{2 \times 35.6} = 26.395505617978 \quad \textbf{(II.8)}$$

$$x_3 = 24.790625492455$$

$$x_4 = 24.738688294075$$

$$x_5 = 24.738633753767$$

In a minimal number of iterations, the solution achieves accuracy to multiple decimal places.

II.2.2 Particle Swarm Optimization "PSO"

II.2.2.1 Overview of PSO

Particle swarm optimization is a method developed from swarm intelligence, which is based on the movement behavior of birds or fish when searching for food. When birds search for food from one place to another, there is always one bird that can sense the food and find the location where it can be found. As if there is a constant exchange of information among them, they will eventually flock to the location where the food can be found. The algorithm proposed by Kennedy and Eberhart in 1995 seeks to simulate this social behavior based on the analysis of the environment and the neighborhood, thus constituting an optimization method by observing the tendencies of neighboring individuals [11]. Each individual seeks to optimize its chances by following a tendency that it moderates through its own experiences. The model they proposed was later extended into a simple and efficient optimization algorithm. **[15]**

$$V_i(k+1) = \omega . V_i(k) + c_1.rand().(pbest_i - X_i(k)) + c_2.rand().(gbest - X_i(k)) \quad \textbf{(II.9)}$$

II.2.2.2 Particle Swarm Optimization (PSO)

Particle swarm optimization relies on a set of individuals initially arranged randomly and uniformly, which we will call particles. These particles move through the search space, each constituting a potential solution. Each particle has a memory of its best visited solution, as well as the ability to communicate with the particles in its surroundings. Based on this information, the particle follows a tendency made up of, on the one hand, its desire to return to its optimal solution, and on the other hand, its imitation of solutions found in its neighborhood. From local optima, the set of particles will normally converge toward the global optimal solution of the problem being addressed **[15]**.

The movement of these particles in a swarm is complex; its dynamics obey specific rules and factors:

- Each individual has a certain "limited" intelligence (which allows it to make a decision).
- Each individual must know its local position and have local information about each individual in its neighbourhood.
- Obey these three simple rules: "stay close to other individuals," "move in the same direction," or "fly at the same speed."

The movement of a particle is influenced by the following three components:

- The particle tends to follow its current direction of movement.
- The particle tends to move toward the best site it has already visited.
- The particle tends to rely on the experience of its neighbors and thus move toward the best site already reached by its neighbors.

All these factors and rules are essential for maintaining cohesion within the swarm, through the adoption of a complex and adaptive collective behavior.

II.2.2.3 Basic PSO Algorithm

Let $f(x)$ be the objective function to be optimized (fitness) and n the number of particles. The essential steps of particle swarm optimization are presented by the following algorithm **[17]**:

1- Random initialization of the population and particle velocities.
2- Determined the best fitness value f at k=0.
3- Processing

Repeat until the end of iteration.

Repeat for each particle.

Generate the new velocity value using equation (II.1).

Calculate the new position using equation (II.2).

Evaluate the fitness value.

Find the best position for each particle.

End.

Find the global best position.

End

The flowchart of the standard PSO is presented in Figure (II.2).

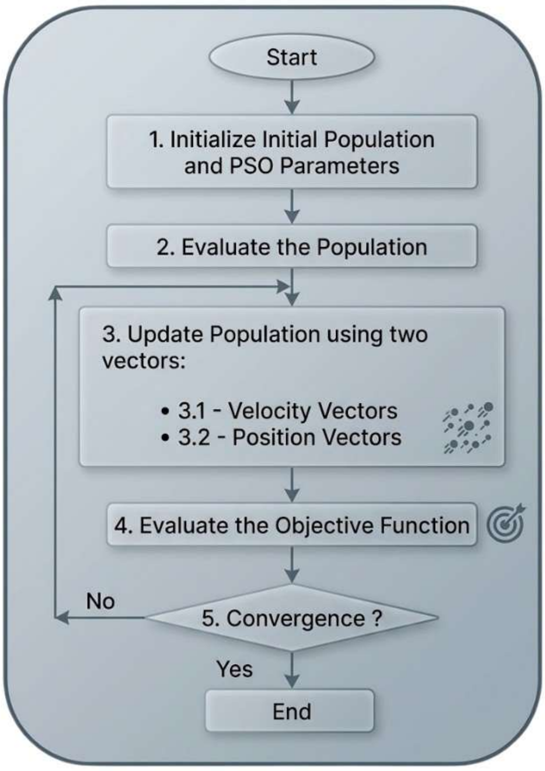

Figure II.3: Flowchart of the PSO algorithm **[18]**

$$I_0^* = \frac{I_{scd}}{e^{\frac{gv_{ocd}}{\eta kT}} - 1}$$

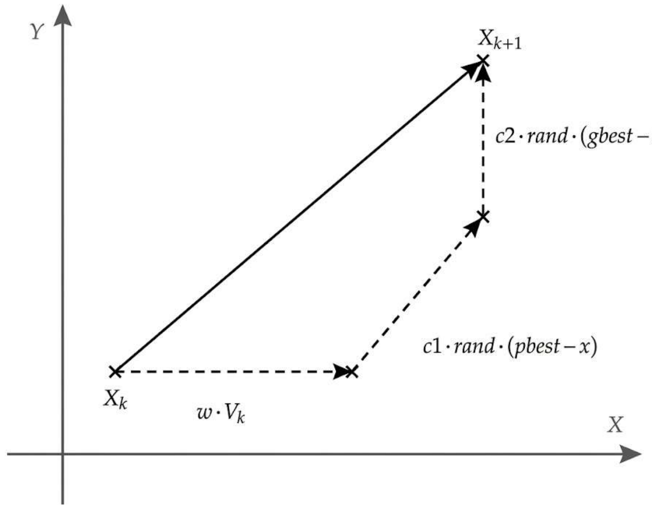

Figure II.4: PSO Position Update.

Utilizing equations (II.7) and (II.8), the fitness function for a single data point is defined as:

$$\boldsymbol{fi} = |\, \boldsymbol{I^*} - \boldsymbol{I_d} \,| \tag{II.10}$$

Within equations (**II.7**), (**II.8**), and (**II.9**), I_0^* is represents the estimated reverse saturation current, $\mathbf{I^*}$ is the calculated load current, $\mathbf{I_d}$ and $\mathbf{V_d}$ are the measured load current and voltage respectively, $\mathbf{I_{scd}}$ is the measured short-circuit current, $\mathbf{V_{ocd}}$ is the measured open-circuit voltage, and $\mathbf{T_d}$ is the recorded ambient temperature. The variables n^*, R_s^*, and R_{sh}^* correspond to the PV parameters targeted for optimiza **[19]**.

Therefore, the comprehensive fitness function evaluating a parameter set across N empirical points is:

$$f = \sqrt{\sum_{i=0}^{N} f_i^2} \tag{II.11}$$

II.2.2.4 Particle and Search Space Definition

For this research, the implemented optimization algorithm seeks the ideal combination of photovoltaic parameters to minimize discrepancies relative to empirical data. Every particle encapsulates a vector containing the parameters targeted for optimization (specifically the diode ideality factor n, series resistance Rs, and shunt resistance Rsh). The boundaries of the search space for these parameters are established relying on practical domain expertise and historical literature **[20]**.

Search Space Boundaries:

• **n:** 0 – 2

• **R_s (Ω):** 0 – 20

• **R_{sh} (Ω):** 10 – 200

II.2.2.5 PSO Implementation

In the implementation of the Particle Swarm Optimization (PSO) algorithm, the Inertia Weight **(ω)** plays a critical role as a strategic mechanism to control the convergence behavior. It functions as a balancing factor between the algorithm's exploration (searching new areas of the solution space) and exploitation (fine-tuning the search around the best-found solutions).

To enhance the search efficiency, a linearly decreasing inertia weight is adopted. At the beginning of the optimization process, a higher value of ω is used to maintain high particle velocities, encouraging global exploration to avoid being trapped in local optima. As the iterations progress, ω is gradually reduced, which "cools down" the particles' momentum, allowing for a more stable and precise local search around the global best position. **[21]**

The dynamic value of the inertia weight is typically calculated using the following linear decay formula:

$$\omega = \omega_{max} - \left(\frac{\omega_{max} - \omega_{min}}{T_{max}}\right) \times t \qquad \textbf{(II.12)}$$

Where:

- ω_{max} **(initially 0.8):** The starting weight, facilitating a broad initial search.
- ω_{min} **(ending at 0.4):** The final weight, ensuring precise convergence in the final stages.

- **t:** The current iteration number.
- **T_{max}:** The maximum number of iterations.

By utilizing this transition from **0.8 down to 0.4**, the algorithm ensures that the particles transition smoothly from a high-energy exploratory state to a high-precision settlement state, significantly improving the accuracy of the extracted photovoltaic parameters **[22]**.

In alignment with standard practices **[23]**, both the cognitive and social acceleration coefficients (**c_1 and c_2**) are configured to 2.0. The velocity limit is constrained to fifty percent of the total search space magnitude across every dimension. The swarm size is established at 50 particles, with the algorithmic termination set at 100 maximum iterations.

A dedicated PSO script intended for the extraction of these PV parameters was coded using MATLAB software **[23]**.

II.3 Fitness function

II.3.1Definition of Fitness Function in PSO

The fitness function is the core of Particle Swarm Optimization (PSO). It is mathematically defined as F: R^D → R, mapping a vector x (particle position in D-dimensional search space) to a numerical value indicating solution quality.

Examples:

- PID control: Mean Square Error (MSE) between desired and actual trajectory
- System identification: MSE combined with Grey Absolute Relational Grade

At each iteration:

1. Fitness value is calculated for each particle.
2. Compare with personal best (pbest) and global best (gbest).
3. Update particle velocity and position to move toward better fitness regions.

The fitness function acts as a compass guiding the swarm toward the optimal solution.

II.3.2 Impact of Fitness Function Choice

Fitness Function Type	Effect on PSO Performance
Single MSE	May be insufficient for complex problems
Cumulative (pbest-based)	Higher convergence quality
Cumulative (swarm-based)	Faster convergence speed
Combined function	Better global exploration, avoids local optima

II.3.3 Recent Advances

1. **FCPSO**: Fitness values dynamically adjust PSO parameters using feedback control.
2. **LBDFs**: Local modification of fitness landscape around stuck particles to escape local optima.

The fitness function defines the "rules of winning" in PSO. Its choice controls the trade-off between convergence speed and solution accuracy. Modern research makes it interactive and adaptive - either using its values to tune the algorithm dynamically or temporarily reshaping it to improve search capability.

Conclusion

Throughout this chapter, we have explored the fundamental principles of system identification in a general context, providing a comprehensive framework for modeling dynamic processes. Specifically, we focused on the detailed implementation of two distinct methodologies for extracting photovoltaic parameters: the Newton-Raphson method as a robust numerical approach, and the Particle Swarm Optimization (PSO) as an intelligent metaheuristic algorithm.

This formulated strategy was deployed to deduce the intrinsic characteristics of PV cells utilizing empirical field data. The validation process confirmed that this identification methodology secures superior parameter precision, maintaining high accuracy despite fluctuations in solar irradiance levels and surrounding ambient temperatures.

In the succeeding chapter, we will transition to the practical application and experimental setup of the PV system. We will demonstrate the integration of the Newton-Raphson method to solve the complex nonlinear equations of the PV panel, while employing the PSO algorithm specifically for the identification and extraction of the optimal parameters. This approach will allow us to validate our model against real-world experimental results, focusing on the single diode model due to its extensive industrial application and reliability.

CHAPTER III

Experimental results and simulation

III.1 Introduction

This chapter highlights Algeria's exceptional solar energy potential, which positions the country as a future leader in renewable energy. With over 3,900 sunshine hours per year in the Sahara and solar irradiation reaching 2263 kWh/m², Algeria is one of the sunniest nations on Earth, making it ideal for solar energy investment.

The chapter covers the scientific fundamentals of solar illumination, including direct, diffuse, and reflected irradiance, as well as the instruments used for measurement. A practical case study is presented from the Applied Research Unit for Renewable Energies (URAER) in Ghardaïa, using the SOLO LINE LX-100M photovoltaic panel. The chapter also discusses experimental methodology, data acquisition, and the advantages of Particle Swarm Optimization (PSO) over traditional numerical methods for PV system modeling.

III.2 Solar Potential of Algeria

Algeria is the largest country in Africa and possesses significant potential in solar energy, making it a promising future investment opportunity. It is one of the sunniest countries in the world, with sunshine exceeding 2,000 hours annually across most of the country. In the Sahara Desert, which comprises a large portion of Algeria, sunshine reaches 3,900 hours per year, as illustrated in Figure 1. Annual solar energy consumption is estimated at 1700 kWh/m^2 in the north and 2263 kWh/m² in the Sahara. This confirms that Algeria is an ideal region for investment in solar energy **[24]**.

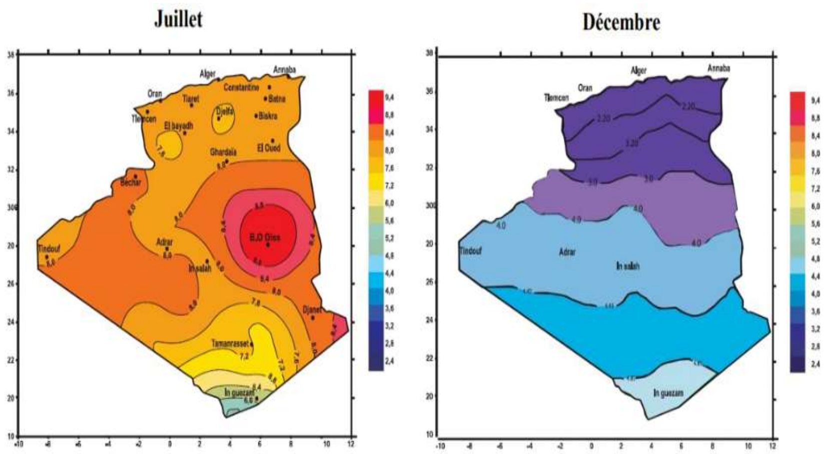

Figure III.1: Solar potential map of Algeria on a horizontal plane **[24].**

III.3 Solar Irradiance

III.3.1 Irradiance

Solar radiation, G, is the energy of sunlight falling on a unit area, and its unit is G = (W/m²). The Earth receives an average of 1.361 kWh/m² of sunlight annually. In addition to atmospheric influences, solar radiation depends on other factors, including: **[25]**

- surface orientation and slope.
- geographical latitude and pollution levels.
- cloud cover characteristics.
- the time of day and season.

III.4 Spectral Distribution of Solar Irradiance

The Sun emits energy as electromagnetic radiation with wavelengths ranging from 0.22µm to 10µm. Figure III.3 shows the spectral distribution of solar radiation. Absorption by the atmosphere is negligible for certain wavelengths but low for visible light between 0.3 and 0.7µm **[26]**.

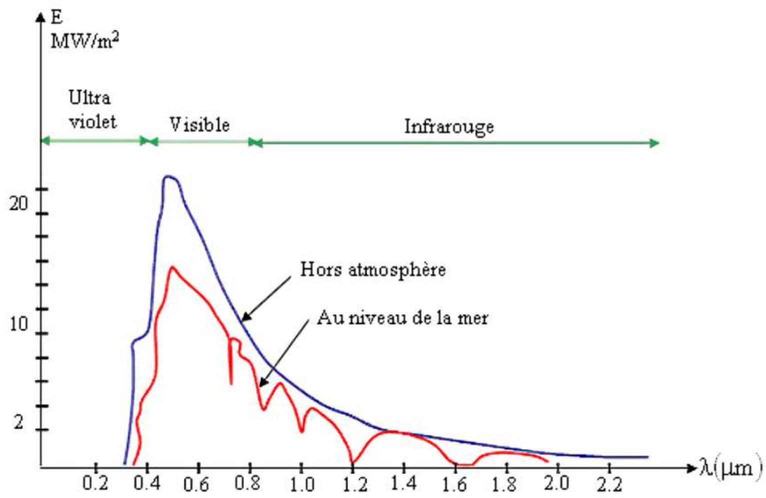

Figure III.2: Spectral distribution of solar radiation outside the atmosphere and at sea level **[26]**.

III.5 Types of Solar Irradiance

III.5.1 Global Irradiance

- Global radiation on a horizontal surface (IGh).
- Global radiation on an inclined surface (IGi) **[27]**.

III.5.2 Direct Irradiance

Direct irradiance represents solar radiation coming through the atmosphere without any deflection or interference. This means the portion coming directly from the direction of the sun. **[28]**.

III.5.3 Diffuse and Reflected Irradiance

Diffuse irradiance is the scattering of direct light through clouds and the atmosphere, while reflected light is due to inclined surfaces. Albedo is the ratio of reflected light to incident light, and it is zero for black objects. **[29]**.

III.6 Irradiation

Solar irradiance, measured in watts per square meter (w/m²), represents the energy received per unit area over a specific period. It depends on several factors, including time of day, cloud cover, duration of sunshine, pollution levels, and latitude. The total annual energy received horizontally is estimated to be between 1400 and 1500 kWh/m² between latitudes 40° North and 40° South. **[30]**.

III.6.1 Hourly Irradiation on a Horizontal Plane

The hourly global irradiation on a horizontal surface is a key parameter for dynamic system modeling.

III.6.2 Daily Irradiation on a Horizontal Plane

The daily global irradiation $G_0(nj)$ is obtained by integrating the hourly values from sunrise to sunset. For a plane inclined at angle β, the daily global irradiation is given by:

$$G_0(h.n_j) = (n_j)[sin(\phi - \beta)\, sin(\delta) + cos(\phi -)\, cos(\delta)]\frac{24}{\pi} I_{SC} W_S W_S \qquad \textbf{(III.1)}$$

Where:

- ϕ = latitude angle
- β = tilt angle
- δ = declination angle
- I_{SC} = solar constant
- W_S = sunset hour angle

III.7 Solar Irradiance Measurement Devices

Solar irradiance G is measured using various instruments **[30]**:

Device	Measurement Type
Pyrheliometer	Direct beam radiation
Pyranometer	Global radiation on a plane
Albedometer	Reflected radiation (albedo)

Figure III.3: Pyrheliometer instrument for direct beam radiation measurement **[31]**.

Figure III.4: Pyranometer instrument for global radiation measurement **[31]**.

Figure III.5: Albedometer for measuring reflected solar radiation **[31]**.

III.8 Geographical Location of Ghardaïa

Ghardaïa is located 600 km south of Algiers, the capital of Algeria, and is considered the gateway to the Algerian Sahara. It serves as a model for studying solar energy, boasting high irradiance levels reaching 75/100. The city receives over 3,500 hours of sunshine annually, with an average daily solar irradiance of 6 kW/m^2 **[34]**.

III.9 Overview of the Renewable Energy Applied Research Unit (URAER)

The Applied Research Unit for Renewable Energies is considered the heart of solar research in Algeria. Located in the Bou Noura Industrial Zone in Ghardaïa, it was established in 1999. It has registered several achievements and patents, in addition to training and mentoring students and engineers. Its departments include:

- Photovoltaic Solar Energy.
- Solar Thermal Energy.
- Wind Energy.
- Energy Systems for Agriculture.

Figure III.6: Photograph of the Renewable Energy Applied Research Unit (URAER) in Ghardaïa.

III.9.1 Photovoltaic Solar Energy Division

The Photovoltaic Solar Energy Department is the largest division within the Applied Research Unit (URAER). Established in 1982, it has undergone several organizational and structural changes. Its objectives include localizing technology, improving the efficiency of desert power plants, and controlling energy conversion and storage systems **[32]**.

III.10 Experimental Data and Methodology

Only 20% of incident sunlight on a PV module is converted to electricity; the rest increases cell temperature, reducing efficiency by 0.4-0.5% per degree rise . A closed-loop water cooling system is proposed to mitigate overheating, improving thermal efficiency **[34]**.

III.10.1 Limitations of Numerical Methods

Numerical methods for parameter estimation are accurate but suffer from:

- Sensitivity to initial guesses
- Complex gradient operations
- Potential singularities during solution **[33]**.

III.10.2 Advantages of Meta-Heuristic Optimization (PSO)

To overcome these limitations, Particle Swarm Optimization (PSO) offers:

- Improved convergence.
- Low sensitivity to initial conditions.
- Absence of singularity issues.
- Use of full I-V curve data rather than critical points only.

III.10.3 Methodology Used

In this study, PV panels are tilted at an angle equal to the local latitude.

Instrumentation: [26].

Sensor Type	Model	Measurement
Thermocouple	K-type with Campbell CS215	Temperature
Pyranometer	Kipp & Zonen CMP21	Solar irradiance

Data acquisition system: Agilent experimental system

Figure III.7: SOLO LINE LX-100M photovoltaic panel installed at URAER with data acquisition instruments.

III.11 Properties of the Photovoltaic Panel

The **SOLO LINE LX-100M** module, manufactured by Luxor, is designed for off-grid applications including:

- Holiday homes and residential systems.
- Solar pumps for irrigation and drinking water.
- Traffic systems, parking meters, and street lighting.
- Telecommunication and measurement systems.

Figure III.8: SOLO LINE LX-100M photovoltaic panel installed at URAER **[33]**.

Table III.3: Datasheet specifications for SOLO LINE LX series photovoltaic modules [33].

Electrical Data	**LX-10P**	**LX-50P**	**LX-100M**	**LX-160P**	**LX-180M**
Rated power P_mpp [Wp]	10	50	100	160	180
Power tolerance	0/+5%	0/+5%	0/+5%	0/+5%	0/+5%
Rated current I_mpp [A]	0.58	2.88	5.39	8.56	9.31
Rated voltage V_mpp [V]	17.39	17.44	18.70	18.73	19.39
Short-circuit current I_sc [A]	0.64	3.24	5.87	9.06	9.75

Electrical Data	**LX-10P**	**LX-50P**	**LX-100M**	**LX-160P**	**LX-180M**
Open-circuit voltage V_oc [V]	21.60	21.60	21.60	22.98	23.05
Max. system voltage [V]	150	400	1000	1000	1000

Table III.4: Temperature coefficients for SOLO LINE LX series [33].

Temperature Coefficient	**LX-10P**	**LX-50P**	**LX-100M**	**LX-160P**	**LX-180M**
Coefficient [P] (%/°C)	-0.49	-0.45	-0.49	-0.45	-0.45
Coefficient [I] (%/°C)	+0.05	+0.05	+0.05	+0.05	-0.05
Coefficient [U] (%/°C)	-0.35	-0.32	-0.35	-0.32	-0.05

Table III.5: Mechanical specifications for SOLO LINE LX series [33].

Specifications	**LX-10P**	**LX-50P**	**LX-100M**	**LX-160P**	**LX-180M**
Cell size (mm)	78×22.5	52×156	125×125	156×156	156×156
No. of cells / type	4×9 / poly	4×9 / poly	4×9 / mono	4×9 / poly	4×9 / mono
Weight (kg)	1.5	5.5	7.8	11.5	11.5
Cable length (mm)	-	850	850	850	850
Cable diameter (mm^2)	-	4	4	4	4

Specifications	LX-10P	LX-50P	LX-100M	LX-160P	LX-180M
Diode	-	-	2×12 A	2×12 A	2×12 A
Junction box IP rating	IP65	IP65	IP65	IP65	IP65

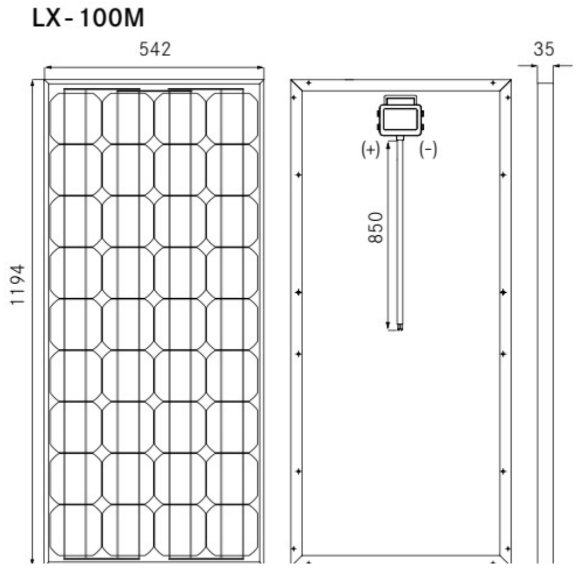

Figure III.9: Mechanical dimensions of the LX-100M photovoltaic module [33].

Conclusion

In conclusion, Algeria possesses tremendous solar resources, particularly in its Saharan regions, where annual sunshine exceeds 3,500 hours and average daily irradiance reaches 6 kW/m^2. These conditions make the country a natural laboratory for solar energy research.

The chapter has emphasized the importance of accurate field measurements using advanced instruments and has provided a solid technical foundation based on the SOLO LINE LX-100M panel specifications. The comparison between numerical and meta-heuristic methods confirms that PSO offers better convergence and reliability. With advanced research facilities like URAER in Ghardaïa, Algeria is well-positioned to advance photovoltaic and renewable energy technologies. The methodologies established here serve as a crucial foundation for the experimental analysis and optimization work in the following chapters.

CHAPTER IV

Results and Discussion

IV.1 Introduction

In this chapter, we will rely on three models to represent the solar cell (ideal model, single diode model and double diode model). These models differ in the number of parameters and degree of complexity, with the aim of comparing the accuracy and ability of these models to represent the real characteristics of the photovoltaic cell.

To work on these models, MATLAB software will be used, which is used to develop mathematical models, apply the PSO algorithm, process experimental data, and plot the electrical curves of the photovoltaic cell. This allows for comparison and evaluation of the results obtained.

IV.2 Experimental results

The following table shows the measurements and results obtained from the URAER testing platform in Ghardaia, for the LX-100M solar panel. This data includes temperature, open-circuit voltage, and current values measured under different operating conditions.

Table IV.1: Experimental measurements obtained from URAER.

Time	Temperature (c)	Vco (volt)	Ir max (A)	V (volt)
10:30	37	21.48	4.87	**61.3**
11:00	38.5	21.16	5.52	**34**
11:30	42	21.19	5.52	**29**
12:00	46	0.63	6.17	**20**
12:30	48	9	6.38	**17**
13:00	58	0.9	6.43	**9**

IV.3 Identification results of LX-100M PV cell model

For all three models, we will examine the calculated current and voltage data, compare them with the actual data, and identify and compare the variables, noting that the process was carried out under the same conditions.

IV.3.1. The current data

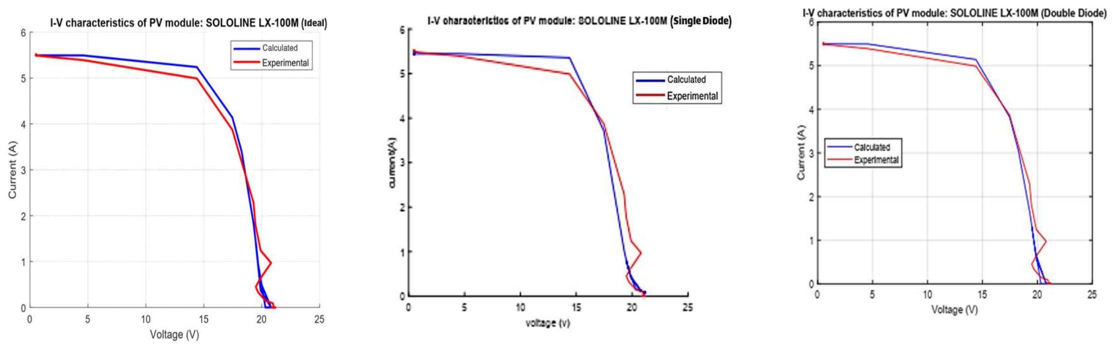

Figure IV.1 : Current curves for the three models.

IV.3.1.1. Analysis and comparison (The current)

As we can see from the Figure IV.1, all models are capable of representing the current curve (I), but with varying accuracy. The ideal model is the least accurate because it neglects many internal losses. The single diode model is relatively more accurate, while the double diode model is the most accurate and consistent with experimental results, making it the best model for representing the behaviour of the solar panel.

IV.3.2. The Power data

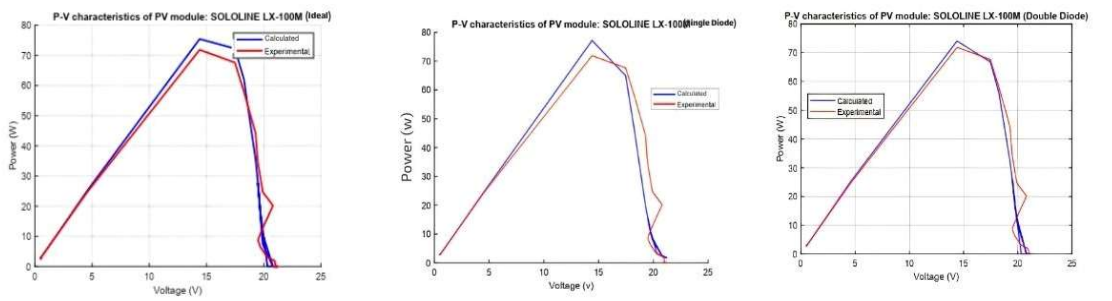

Figure IV.2 : Power curves for the three models.

IV. 3.2.1. Analysis and comparison (The power)

We can see from the Figure IV.2 that the power curve representation varies from one model to another due to losses and influencing resistances. The ideal model is the weakest among them, while the single-diode model is better and slightly more accurate.

However, the double-diode model is the best and gives the most accurate and successful representation due to its precise design.

3.3. The RMSE data

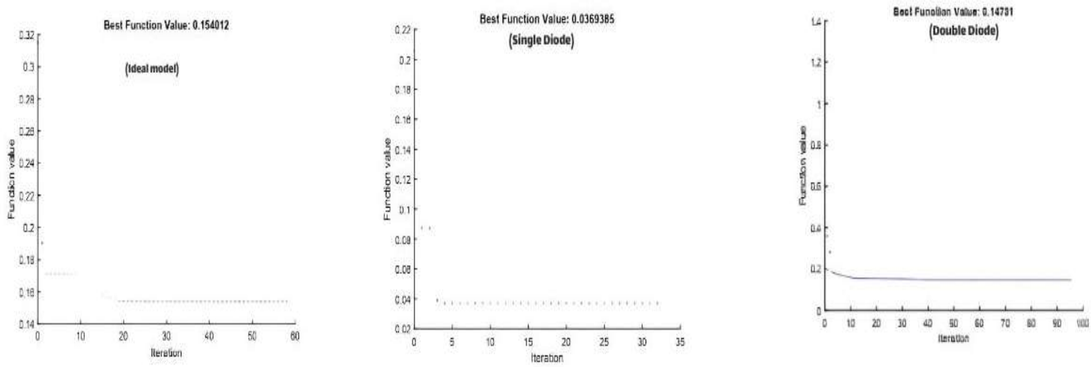

Figure IV.3: RMSE for the three models.

IV.3.3.1. Analysis and comparison (The RMSE)

The lower the RMSE value in the model, the better the model. As shown in Figure IV.3, the single-diode model gives the best result, making it the most successful among the models used.

IV.4 The result of the three models

	models		
Parametres	**Ideal**	**Single diode**	**Double diode**
I_{ph} (A)	5.49	5.87	5.5
I_{s1} (A)	0.0001	0	0.0001
I_{s2} (A)	/	/	0
n_1	1.98	1	1.99
n_2	/	/	1.98
R_s (ΩΩ)	0	0.4289	0.0035
R_{sh} (Ω Ω)	/	500	50
RMSE	0.154	0.0369	0.1473

IV.4.1. Summary of results

Based on our observations and relying on these results, we find that the single-diode model is the best among the other models and is the closest to representing the behavior of the solar panel.

Conclusion

In this chapter, three photovoltaic cell models were applied to the LX-100M solar panel based on available URAER values. The actual current was compared to the calculated current for each model after determining its parameters using the PSO algorithm. The results showed that the models were able to represent the electrical behavior of the solar panel with varying degrees of accuracy, and the dual-diode model was found to be the most consistent with the experimental data.

General Conclusion

General Conclusion

The work presented in this thesis successfully achieved its primary objective: the comparative identification of photovoltaic model parameters using experimental data and the Particle Swarm Optimization (PSO) algorithm. Based on real I-V measurements taken from the LX-100M solar panel at the URAER research unit in Ghardaïa, three models-ideal, single-diode (SDM), and double-diode (DDM)—were developed, simulated in MATLAB, and rigorously evaluated.

The results clearly demonstrate that while all models can represent the electrical behavior of the PV panel to some extent, their accuracy varies significantly. The ideal model, which neglects internal losses, proved insufficient for precise simulation. The single-diode model offered a good balance between accuracy and computational simplicity, achieving a root mean square error (RMSE) of 0.0369. However, the double-diode model provided the highest fidelity to experimental data, particularly at low irradiance levels, with an RMSE of 0.1473-though at the cost of increased computational complexity due to its seven parameters.

The PSO algorithm proved to be highly effective for this nonlinear identification problem, demonstrating strong convergence properties and low sensitivity to initial conditions compared to classical numerical methods. The experimental methodology, grounded in real Saharan climate conditions, adds practical value to the findings.

In conclusion, the choice of PV model depends on the application: the SDM is recommended for real-time or resource-constrained systems where speed is critical, while the DDM is preferable for high-precision offline simulations and performance analysis under variable irradiance. Future work may extend this comparison to other metaheuristic algorithms (e.g., genetic algorithms, grey wolf optimizer) and explore adaptive PSO variants for dynamic parameter tracking under rapidly changing weather conditions. This research contributes a reproducible framework for PV model identification and offers actionable insights for solar energy practitioners in sun-rich regions like Algeria.

References

References

[1] Messenger, R., & Ventre, J. (2010). *Photovoltaic Systems Engineering* (3rd ed.). CRC Press.

[2] Boyle, G. (2012). *Renewable Energy: Power for a Sustainable Future* (3rd ed.). Oxford University Press.

[3] Duffie, J. A., & Beckman, W. A. (2013). *Solar Engineering of Thermal Processes* (4th ed.). Wiley.

[4] Othmane Benseddik, Fathi Djaloud, " Study and optimization of the operation of a photovoltaic system", master's thesis, Kasdi Marbah-Ouargla University, 2012

[5] U.S. Department of Energy (DOE), Office of Energy Efficiency & Renewable Energy. "Solar Photovoltaic Cell Basics." Available at: energy.gov. *OR*

[6] Green, M. A. (2003). *Third Generation Photovoltaics: Advanced Solar Energy Conversion*. Springer.

[7] Nelson, J. (2003). *The Physics of Solar Cells*. Imperial College Press.

[8] Duffie, J. A., & Beckman, W. A. (2013). *Solar Engineering of Thermal Processes* (4th ed.). Wiley.

[9] Nelson, J. (2003). *The Physics of Solar Cells*. Imperial College Press.

[10] Boyle, G. (2012). Renewable Energy: Power for a Sustainable Future (3rd ed.). Oxford University Press.

[11] Würfel, P., & Würfel, U. (2016). *Physics of Solar Cells: From Principles to New Concepts*. Wiley-VCH.

[12] Duffie, J. A., & Beckman, W. A. (2013). *Solar Engineering of Thermal Processes*. John Wiley&Sons.

[13] Y. Shi and R. Eberhart, "A modified particle swarm optimizer," Proceedings of the IEEE International Conference on Evolutionary Computation, Anchorage, AK, USA, 1998, pp. 69-73.

[14] J. Kennedy and R. Eberhart, "Particle swarm optimization," Proceedings of ICNN'95 - International Conference on Neural Networks, Perth, WA, Australia, 1995, vol. 4, pp. 1942-1948.

[15] K. Ishaque and Z. Salam, "An improved particle swarm optimization (PSO) algorithm for solar PV parameter extraction," Applied Energy, vol. 88, no. 11, pp. 4267-4276, 2011.

[16] A. R. Jordehi, "Parameter estimation of solar photovoltaic (PV) cells: A review," Renewable and Sustainable Energy Reviews, vol. 61, pp. 354-371, 2016.

[17] M. G. Villalva, J. R. Gazoli, and E. R. Filho, "Comprehensive approach to modeling and simulation of photovoltaic arrays," IEEE Transactions on Power Electronics, vol. 24, no. 5, pp. 1198-1208, 2009.

[18] J. C. Bansal et al., "Inertia weight strategies in particle swarm optimization," Third World Congress on Nature and Biologically Inspired Computing (NaBIC), Salamanca, Spain, 2011, pp. 633-640.

[19] A. M. Humada et al., "Solar cell parameters extraction techniques: A review," Renewable and Sustainable Energy Reviews, vol. 56, pp. 350-371, 2016.

[20] S. C. Chapra and R. P. Canale, Numerical Methods for Engineers, 7th ed. New York: McGraw-Hill Education, 2015.

[21] A. Askarzadeh and A. Rezazadeh, "Extraction of maximum power point in solar cells using bird mating optimizer-based parameters identification," Solar Energy, vol. 90, pp. 123-133, 2013.

[22] I. Dincer, "Renewable energy and sustainable development: a crucial review," Renewable and Sustainable Energy Reviews, vol. 4, no. 2, pp. 157-175, 2000.

[23] J. Twidell and T. Weir, Renewable Energy Resources, 3rd ed. London: Routledge, 2015.

[24] Bouchouicha. k. Modélisation multi spectrale des images satellitaire, application quantification du bilan d"énergie sol-atmosphère. Thèse de Doctorat en science. Université Mohammed Boudiaf, Oran 2017.

[25] " Matlab/Simulink Tutorial", School of Electrical, Electronic and Computer Engineering, Release 13, Version 6.5, 2nd Edition, 2003.

[26] Fatiha, Y., optimisation d‟un système solaire de production de l‟eau chaude Décembre 2009., Ecole Nationale Polytechnique 10, Avenue Hassen Badi, El-Harrach, ALGER.

[27] " MesriMokhtaria& Professeur Cheknane Ali Introduction au gisement Solaire algérien Th".

[28] F. Kasten, " A Simple Parameterization of Two Pyrheliometric formulae for determining the Linke Turbidity Factor", Meteorology Rdsch, Vol. 33, pp. 124 - 127, 1980.

[29] K.Feussner and P. Dubois, „Trübungsfaktor, Precipitable Water‟, Staub. GerlandsBeitr., Geophysical, Vol. 27, pp. 132 - 175, 1930.

[30] A. Louche, G. Peri and M. Iqbal, „An analysis of Linke Turbidity Factor‟, Solar Energy, Vol.37, N°6, pp. 393 – 396, 1986.

[31] F. Kasten, „The Linke Turbidity Factor Based on Improved Values of the Integral Rayleigh Optical Thickness‟, Solar Energy, Vol. 56, N°3, pp. 239 – 244, 1996.

[32] J.R.Vaillant, « Des recours immédiats à l‟énergie solaire contre la pénurie d‟énergie et la hausse des prix », Ed. Eyrolles, France, 1980.

[33] Magister BAISSI Mohamed Tahar Etude théorique et expérimentale des paramètres de fonctionnement d‟un capteur solaire plan Université Mohamed Khider – Biskra 28/06/2012.

[34] Fatiha Yettou, Malek Ali, Mourad Haddadi, Amor Gama, Etude comparative de deux modèles de calcul du rayonnement solaire par ciel clair en Algérie, January 2009.

[35] the official site of www.cder.dz.